Optimization of solar photovoltaic and battery energy storage system for peak demand reduction under Malaysia's new tariff structure

Lek Keng Lim, Wai Shin Ho*, Zarina Ab. Muis, Zhen Quan Wong

Process Systems Engineering Centre (PROSPECT), Faculty of Chemical and Energy Engineering, Universiti Teknologi Malaysia, 81310 Johor Bahru, Johor, Malaysia

ABSTRACT

Malaysia has introduced a new electricity tariff structure that increases the charge for maximum demand. Other than using solar photovoltaic (PV) systems to reduce energy costs, a battery energy storage system (BESS) is required to perform peak shaving and optimize the building's energy usage. Previous studies mainly focused on utilizing solar PV or BESS to supply energy during night-time periods, with limited investigation into peak demand management. This study develops a mixed-integer linear programming (MILP) model in General Algebraic Modelling System (GAMS) to formulate an integrated energy management framework that coordinates solar generation, BESS operation, and grid interaction. The model aims to minimize the total energy system cost while ensuring reliable energy supply for the building. Results show that the optimum configuration of solar PV and BESS can reduce grid energy consumption and peak demand by up to 15%, while excessive peak shaving beyond the optimum point is not economically feasible due to high battery investment.

1. Introduction

In 2025, Malaysia has revised its electricity tariff structure [1], increasing the charge for maximum demand while shortening the duration of the peak hour period from 8 a.m.-10 p.m. to 2 p.m.-10 p.m. This change encourages consumers to manage their peak demand more efficiently in order to avoid higher demand charges. Previously, strategies to reduce electricity costs mainly relied on renewable energy integration, particularly solar photovoltaic (PV) systems, to decrease energy consumption from the grid. However, under the new tariff structure, reducing total energy usage alone is not sufficient. A battery energy storage system (BESS) is now required to limit peak demand and optimise the building's energy profile [2].

The integration of a battery energy storage system (BESS) with solar photovoltaic (PV) generation enables a synergistic approach to both energy cost reduction and peak demand management. The hybrid configurations enhance the flexibility and reliability of the building's energy system by enabling temporal energy shifting and load levelling [3]. To ensure the optimal coordination of solar generation, battery charging and discharging, and grid interaction, a mathematical optimisation framework is required. In contrast to previous studies that primarily concentrated on minimising the total energy drawn from the grid [4,5], the present work emphasises the optimisation of system operation to minimise maximum demand while maintaining the overall reliability and energy supply adequacy of the building.

This study develops a mixed integer linear programming (MILP) mathematical model to formulate the energy management system problem integrated with both solar PV and BESS. The objective of the model is to minimise the overall cost of the energy system by reducing maximum demand without compromising the energy requirements of the building.

2. Materials and methods

Equation (1) is the objective function, representing the summation of all costs. The costs include solar panel cost, battery capacity cost, battery power cost, maximum demand cost, and grid energy cost. Equation (2) determines the solar panel cost, which is the number of solar panels installed multiplied by the solar panel unit cost. Equation (3) determines the battery capacity cost by multiplying the battery capacity by the battery capacity unit cost. Other than the capacity cost, there is another cost related to the battery, namely the battery power cost, which accounts for the battery charging and discharging rate. Equation (4) determines the battery power cost by multiplying the battery power by the battery power unit cost. Equation (5) determines the maximum demand cost from the national grid. The grid power is multiplied by the maximum demand unit cost defined by the national grid tariff. Equation (6) determines the grid energy cost when purchasing energy from the grid. The grid energy cost is calculated by multiplying the grid energy by the time-of-use tariff, which has peak and off-peak rates. All capital cost is annualized by putting in the annualized unit cost.

*Corresponding author
Email address: hwshin@utm.my*

$$Cost^{Total} = Cost^{Solar} + Cost^{Batc} + Cost^{BatP} + Cost^{Power} + Cost^{Grid} \tag{1}$$

$$Cost^{Solar} = Solar^{NumPanel} \times Cost^{SolarU} \tag{2}$$

$$Cost^{Batc} = Bat^{Cap} \times Cost^{BatCU} \tag{3}$$

$$Cost^{BatP} = Bat^{Power} \times Cost^{BatPU} \tag{4}$$

$$Cost^{Power} = Grid^{Power} \times Cost^{PowerU} \times 12 \tag{5}$$

$$Cost^{Grid} = \sum_{D,T} GridEnergy_{T,D} \times Tariff_T \times Day_D \tag{6}$$

Equation (7) shows how the demand is fulfilled by different energy sources. The energy sources include grid energy to demand, solar energy, and energy discharged from the battery. Equation (8) shows the allocation of grid energy purchase, whether it goes to the battery or directly to the demand. Equation (9) determines the maximum power demand, representing the highest power level during the peak hour.

$$Demand_{T,D} = Grid_{T,D}^{Demand} + Solar_{T,D}^{Demand} + Bat_{T,D}^{Demand} \tag{7}$$

$$Grid_{T,D}^{Energy} = Grid_{T,D}^{Battery} + Grid_{T,D}^{Demand} \tag{8}$$

$$Grid_{T,D}^{Energy} \times Bin_T^{Peak} \leq Grid^{Power} \tag{9}$$

Equation (10) determines the amount of solar energy produced by the solar PV, calculated by multiplying the solar panel area with the solar panel efficiency and the solar irradiation. Equation (11) shows the area of the solar panel by multiplying the number of solar panels by the area of each solar panel.

$$Solar_{T,D}^{Energy} = Solar^{Area} \times Solar^{Eff} \times Solar_{(T,D)}^{Irr} \tag{10}$$

$$Solar^{Area} = Solar^{NumPanel} \times Solar^{AreaPanel} \tag{11}$$

$$Solar^{Area} \leq Solar^{MaxArea} \tag{12}$$

Equation (13) determines the energy charged into the battery by summing the solar energy to the battery and the grid energy to the battery, multiplied by their respective charging losses. Equation (14) determines the energy supplied from the battery to meet the demand, including the discharging loss. Equation (15) determines the energy for fulfilling the demand after deducting the battery discharging efficiency. Equation (16) determines the usable battery capacity by multiplying the battery capacity by the depth of discharge. Equations (17) and (18) identify the battery charging and discharging rates.

$$Bat_{T++1,D}^{SOC} = Bat_{T,D}^{SOC} + Bat_{T,D}^{in} - Bat_{T,D}^{Out} - Bat^{EffLoss} \times Bat_{T,D}^{SOC} \tag{13}$$

$$Bat_{T,D}^{in} = Solar_{T,D}^{Battery} \times Bat^{CharEff} + Grid_{T,D}^{Battery} \times Bat^{CharEff} \times Bat^{ACDC} \tag{14}$$

$$Bat_{T,D}^{Out} \times Bat^{DisEff} = Bat^{Demand(T,D)} \tag{15}$$

$$Bat_{T,D}^{SOC} \leq Bat^{Cap} \times Bat^{DOD} \tag{16}$$

$$Bat_{T,D}^{in} \leq Bat^{Power} \tag{17}$$

$$Bat_{T,D}^{out} \leq Bat^{Power} \tag{18}$$

Equation (19) shows the equation for annualizing the solar and battery CAPEX. The annualisation factor is to annualise the solar and battery CAPEX into an annual fee to have a better comparison with the operation cost.

$$Annualisation\ Factor = \frac{IR((1 + IR)^{LT})}{(1 + IR)^{LT} - 1} \tag{19}$$

Figure 1 illustrates the energy demand profile of Building N01A, an office building located at the UTM FKT campus. The demand begins to rise at around 7 a.m. as occupants arrive and electrical systems such as lighting, air conditioning, and office equipment are switched on. The load reaches approximately 50 kWh and remains relatively stable throughout the working hours until about 4 p.m. After office activities wind down, the load gradually decreases through 5 p.m. and 6 p.m., before dropping significantly after 7 p.m. The demand then stabilises at around 5 kWh during the night, which reflects the operation of essential services such as security systems, standby equipment, and basic building loads. This pattern clearly corresponds to the building's operating hours of 8:00 a.m. to 5:30 p.m., demonstrating that occupancy behaviour is the primary driver of electricity usage.
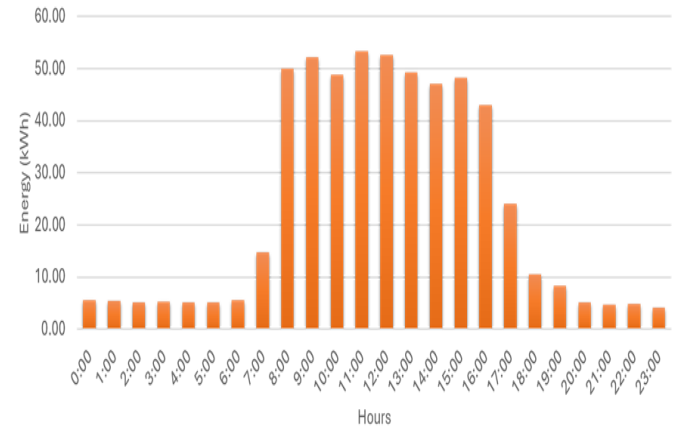

Figure 1. Energy demand of N01a UTM.

Table 1 presents the different scenarios analysed in this study, defined based on the maximum power demand limits of the building. The original condition (Pori) represents the existing operation of the building with a maximum power demand of 48.2 kW and no energy optimisation applied. The optimum case (Popt) represents the power level determined by the mathematical model that minimises the total system cost while maintaining supply reliability. Scenarios P0, P10, P20, P30, and P40 represent controlled maximum power demand limits of 0 kW, 10 kW, 20 kW, 30 kW, and 40 kW, respectively. Each scenario simulates a different level of peak shaving to evaluate the impact on system performance, battery capacity, and economic feasibility.

Table 1. Scenario Description

	Opt	POri	P0	P10	P20	P30	P40
Maximum power demand (kW)	Variable	48.2	0	10	20	30	40

Table 2 presents the tariff structure applied in this study, based on TNB's latest medium-voltage commercial building tariff. The tariff consists of two cost mechanisms: energy charges and maximum demand charges. The energy charge is divided into peak and off-peak periods, where the peak tariff is RM 0.3132/kWh (applicable from 2:00 p.m. to 10:00 p.m.), and the off-peak tariff is RM 0.2723/kWh. The maximum demand charge, amounting to RM 97.06 per kW, is imposed on the highest power demand recorded within the billing period.

Table 2. Malaysia Tariff Structure

Tariff	Cost
Peak hour tariff	0.3132 RM/kWh per month
Off-peak hour tariff	0.2723 RM/kWh per month
Maximum demand	97.06 RM/kW per month

As shown in Table 3, the cost and technical parameters of the solar photovoltaic (PV) system are summarised. The unit cost of the solar panel is 301.40 RM per unit, with an efficiency of 22% and an area requirement of 2.702 m² per panel. Solar maximum area is based on the site limitation, which is roof area in this case study.

Table 3. Solar PV system Information

Solar annualized unit cost	301.40 RM/unit/year
Solar efficiency	22 %
Area per solar panel	2.702 m^2/unit
Solar max area	100 m^2
Solar PV panel cost	3000 RM/unit
Solar panel lifetime	12
Interest rate	3 %
Capital recovery factor solar panel	0.100

As shown in Table 4, the battery energy storage system (BESS) has a unit cost of 213.69 RM per kWh and a rated power of 7.13 kW per unit. The charging and discharging efficiencies are both 90%, with a self-discharge loss of 0.0042%. An inverter loss of 5% is also considered. These values are used in the model to estimate the battery cost and performance when integrated with the solar PV system.

Table 4. Battery System Information

Battery annualized unit cost	213.69 RM/kWh
Battery power unit	7.13
Battery charging efficiency	90%
Battery discharging efficiency	90%
Self-discharge loss	0.0042%
Inverter loss	5%
Battery unit cost	1500 RM/unit
Battery lifetime	8
Interest rate	3%
Capital recovery factor battery	0.142

3. Results and discussions

The problem is formulated in MILP and solved by using the CPLEX solver in GAMS. The solver status is optimal with an execution time of 0.063 seconds using a laptop with AMD Ryzen 7 7435HS (3.1GHz) and 16 GB RAM. The model statistics consist of 40 blocks of equations, 1032 single equations, 747 single variables, 2,662 non-zero elements, and 103 discrete variables.

Figure 2 illustrates the relationship between the required battery capacity and the maximum grid power demand for seven different scenarios, namely P0, P10, Opt, P20, P30, P40, and Pori. The blue line represents the grid power, while the orange line shows the corresponding battery capacity required for each case.
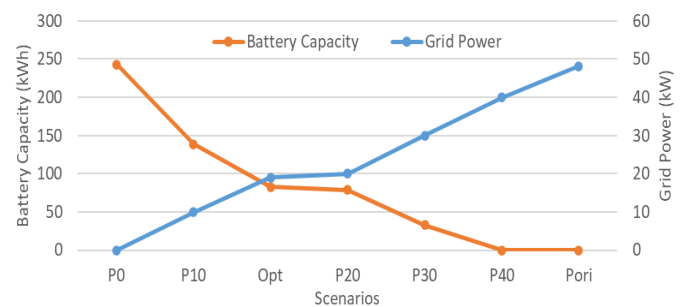
Figure 2. Battery capacity and grid maximum power demand for case studies.

As observed, when the grid power limit is reduced, the battery capacity requirement increases significantly. In the original condition (Pori), the building operates at a maximum demand of approximately 49 kW without any battery support. Under the optimum case determined by the model (Popt), the grid power decreases to around 19 kW with moderate battery use. When the grid limit is set to 40 kW, the solar PV system still provides sufficient energy, and only a small battery capacity is needed. However, as the limit is further reduced to 30 kW, 20 kW, and 10 kW, the required battery capacity increases sharply to approximately 33 kWh, 79 kWh, and 139 kWh, respectively. In the zero-grid case (P0), a full battery capacity of about 243 kWh is required to meet the entire load. This trend indicates a non-linear, exponential relationship between peak demand reduction and battery capacity. The

higher the peak shaving target, the greater the battery investment required, which highlights the importance of identifying an economically feasible operating point through optimisation.

Figure 3 and Figure 4 show the percentage contribution of solar, grid, and battery energy sources under sunny-day and rainy-day conditions, respectively. In the optimum case, about 20% of the total energy comes directly from solar PV, while around 5% is supplied from the battery. The battery energy is stored from solar generation during non-peak hours or from grid electricity purchased during off-peak periods. In P0 and P10, grid usage is relatively low because both solar and grid energy are mainly utilised to charge the battery, resulting in higher battery usage and a larger required battery capacity. The P20 case demonstrates an energy distribution similar to the optimum scenario, showing a balanced operation between solar and battery use. For P30 and P40, battery utilisation becomes limited as the available solar generation during peak hours is sufficient to meet the building's energy demand.
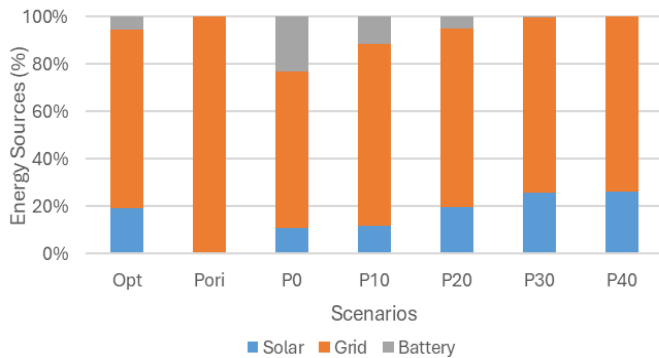

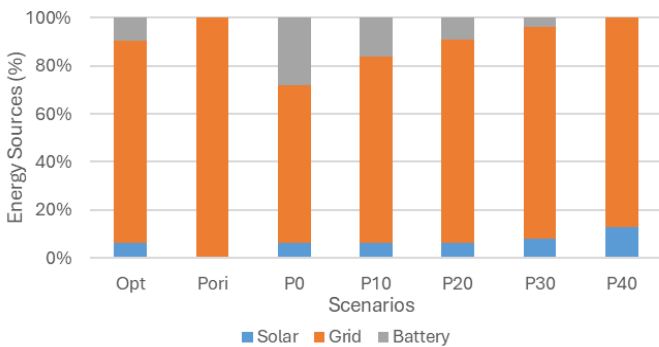**Figure 3.** Energy sources of each scenario during sunny day.

Figure 4. Energy sources of each scenario during rainy day.

Under rainy-day conditions, the overall energy usage pattern remains similar to that of sunny days. However, the contribution of solar energy decreases while battery utilisation increases. This highlights that the battery system becomes more critical during low solar generation periods, directly influencing the required battery sizing. Overall, the results indicate that battery utilisation is highest when grid power is highly restricted, while solar contribution remains relatively consistent across most scenarios. The coordinated operation between solar PV and the BESS enables efficient energy management and reduces dependence on grid electricity.

Figure 5 illustrates the optimum hourly energy profile of the building, showing how energy from different sources is used to meet the total demand. The yellow bars represent energy supplied directly from the grid, the blue bars show energy supplied directly from solar PV, the orange bars indicate solar energy stored in the battery and later discharged to meet demand, and the grey bars represent grid energy stored in the battery and later used for demand.
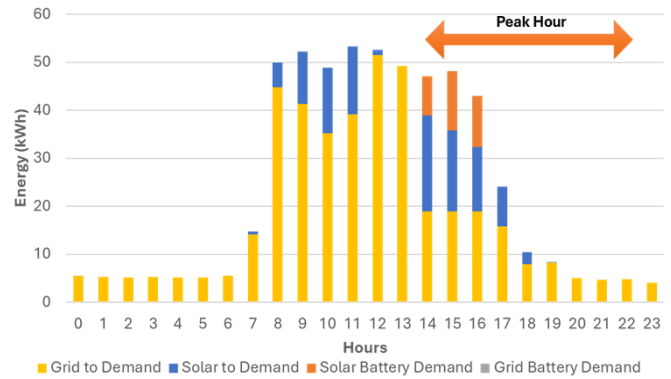

Figure 5. Hourly energy profile of the building for case OPT during sunny day.

The solar PV system begins generating usable energy at around 8 a.m. and continues until approximately 11 p.m. During midday (around 12 p.m. to 1 p.m.), solar generation is stored in the battery instead of being used directly to supply demand. This stored energy is later discharged during the peak-hour period (2 p.m. to 10 p.m.) to reduce grid dependency. During the peak hours, both direct solar power and battery discharge contribute to fulfilling the building's energy demand. This coordinated use of solar and battery energy effectively reduces the maximum demand from the grid, improving the overall efficiency and cost performance of the energy system.

Figure 6 presents the optimum hourly energy profile of the building during rainy-day conditions. In the morning period, all available solar energy is directed to charge the battery rather than being used immediately for demand. The stored energy is then discharged during the peak-hour period to help reduce the maximum grid demand. However, due to reduced solar irradiation, the solar energy generated is insufficient to fully meet the building's energy demand. As a result, the battery is partially charged using grid electricity during off-peak hours to ensure sufficient energy availability during peak periods. This coordinated operation between solar, battery, and grid sources maintains supply reliability and minimizes peak demand under limited solar conditions.
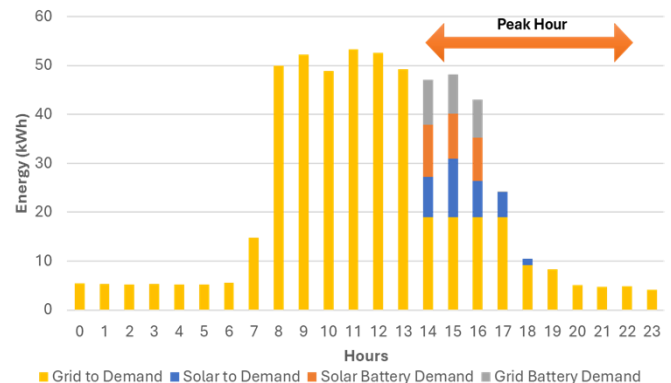

Figure 6. Hourly energy profile of the building for case OPT during rainy day.

Figure 7 and Figure 8 present the hourly energy profiles of the P0 case under sunny-day and rainy-day conditions. During sunny days, all solar energy generated is stored in the battery for use during the peak-hour period. Between 2 p.m. and 6 p.m., the energy supply is relatively balanced, with approximately 40% of the demand met directly by solar power, while the remaining portion is supplied from the battery. The battery energy in this case is derived from both stored solar generation and grid electricity that was charged during off-peak hours. Compared with the previous figure, the contribution from the battery increases significantly, resulting in a much larger required battery capacity.
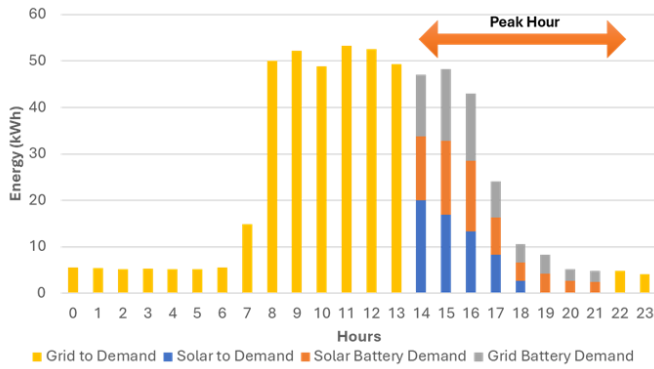

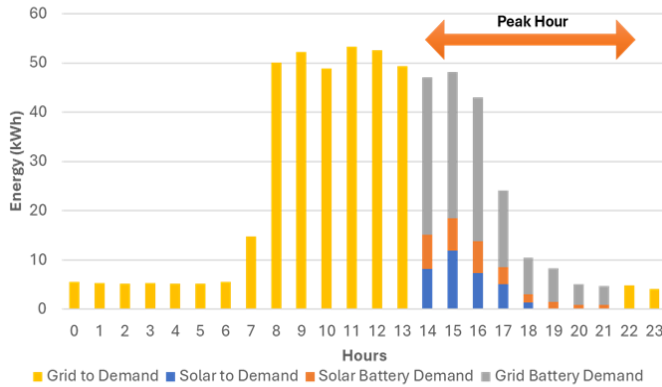**Figure 7.** Hourly energy profile of the building for case P0 during sunny day.

Figure 8. Hourly energy profile of the building for case P0 during sunny day.

Under rainy-day conditions, the direct solar contribution decreases sharply, and the system relies heavily on stored battery energy to meet demand. Due to the limited solar irradiation, less solar energy is available for battery charging, causing most of the stored energy to come from the grid during off-peak periods. This condition highlights the importance of sufficient battery capacity and effective charging management to ensure a stable energy supply during periods of low solar generation.

Table 5 presents the capital expenditure (CAPEX), operational expenditure (OPEX), and total annual cost for different scenarios. The CAPEX and OPEX are annualised based on their lifetime and interest rate. The solar installation cost remains the same for all cases because the system maintains maximum solar capacity installation to achieve greater energy savings. The overall cost variation mainly depends on the battery capacity, power rating, and the maximum power demand cost.

Table 5. Overall Cost of each Scenario

	Opt	Pori	P0	P10	P20	P30	P40
Capital Cost							
Solar Cost	11151	0	11151	11151	11151	11151	11151
Battery Capacity Cost	17736	0	51925	29702	16881	7052	0
Battery Power Cost	158	0	308	229	150	71	0
Total Annualized CAPEX	**29045**	**0**	**63385**	**41083**	**28182**	**18274**	**11151**
Operation Cost							
Power Cost	22152	56144	0	11647	23294	34942	46589
Energy Cost	46023	58372	47360	46387	45992	45712	45646
Total Annualized OPEX	**68175**	**114516**	**47360**	**58034**	**69286**	**80654**	**92235**
Total Annual Cost	**97220**	**114516**	**110745**	**99116**	**97469**	**98927**	**103386**

The power cost decreases almost linearly as the maximum power demand is reduced through higher battery utilisation. However, the battery cost does not follow a linear pattern and increases sharply when more power shaving is targeted because a larger battery capacity is required. The original condition (Pori) records the highest total annual cost due to full reliance on grid electricity without any solar or battery support.

Among all cases, the total cost decreases steadily until the P20 case, which achieves a balance between solar use, battery size, and power demand reduction. After the optimum condition (Popt), the total cost increases again for P10 and P0, as the additional investment in battery capacity outweighs the savings from the reduced maximum power demand charges. This finding shows that excessive peak shaving beyond the optimum point is not economically favourable.

4. Conclusions

This study demonstrates the potential of integrating a battery energy storage system (BESS) with solar photovoltaic (PV) generation to address the challenges introduced by Malaysia's revised electricity tariff structure. The proposed mixed-integer linear programming (MILP) model effectively coordinates solar generation, battery operation, and grid interaction to minimise total system cost while maintaining supply reliability. The modelling results confirm that combining solar PV and BESS enables both grid energy reduction and significant peak demand shaving, achieving up to a 15% improvement in overall performance. The findings also reveal that beyond the optimum configuration, further

peak shaving results in diminishing economic returns due to the rapidly increasing cost of battery capacity. These insights highlight the importance of identifying a balanced design between solar utilisation, battery investment, and tariff response. Future work should include real-time control validation and sensitivity analysis to evaluate the influence of varying tariff structures, battery degradation, and weather conditions on long-term system performance.

Acknowledgment

References

[1] Sunview | Empowering Sustainability with Sunview Solar Solutions [Internet]. TNB tariff restructure non-domestic: everything you need to know (effective 1 July 2025); 2025 Jul. Available from: https://www.sunview.com.my/r/tnb-tariff-restructure-non-domestic-everything-you-need-to-know-effective-1-july-2025

[2] Zahari NE, Mokhlis H, Mubarak H, Mansor NN, Sulaima MF, Ramasamy AK, Zulkapli MF, Ja'apar MA, Jaafar M, Marsadek M. Integrating solar PV, battery storage, and demand response for industrial peak shaving: a systematic review on strategy, challenges and case study in Malaysian food manufacturing. IEEE Access [Internet]. 2024:1. Available from: https://doi.org/10.1109/access.2024.3420941

[3] Abbass A. Hybrid renewable energy microgrid optimization: an analysis of system performance and cost-efficiency using Python-generated custom code for Diesel-wind-solar configurations. Energy Storage Sav [Internet]. 2025 Aug. Available from: https://doi.org/10.1016/j.enss.2025.07.001

[4] Khosravani A, DeHaan M, Billings BW, Powell KM. Electrification of residential and commercial buildings integrated with hybrid renewable energy systems: a techno-economic analysis. Energy [Internet]. 2024 Sep;302:131893. Available from: https://doi.org/10.1016/j.energy.2024.131893

[5] Krarouch M, Allouhi A, Hamdi H, Outzourhit A. Energy, exergy, environment and techno-economic analysis of hybrid solar-biomass systems for space heating and hot water supply: Case study of a Hammam building. Renew Energy [Internet]. 2024 Jan:119941. Available from: https://doi.org/10.1016/j.renene.2024.119941